

## Gravity currents over porous substrates

By L. P. THOMAS<sup>†</sup>, B. M. MARINO<sup>†</sup> AND P. F. LINDEN

Department of Applied Mathematics and Theoretical Physics, University of Cambridge,  
Silver Street, Cambridge CB3 9EW, UK

(Received 18 July 1997 and in revised form 24 November 1997)

Results of laboratory experiments are presented in which a fixed volume of homogeneous fluid is suddenly released into another fluid of slightly lower density, over a horizontal thin metallic grid placed a given distance above the solid bottom of a rectangular-cross-section channel. Dense liquid develops as a gravity current over the grid at the same time as it partially flows downwards. The results show that the gravity current loses mass at an exponential rate through the porous substrate with a time constant  $\tau$ ; the front velocity and the head of the current also decrease exponentially. The loss of mass dominates the flow and, in contrast to gravity currents running over solid bottoms, no self-similar inertial regime seems to be developed. A simple model is introduced to explain the scaling law of the loss of mass and the evolution of the front position. The flow evolution depends on the characteristic time of the initial (slumping) phase and the time constant  $\tau$ , related to the initial conditions and the permeability of the porous substrate, respectively. Qualitative comparisons with other gravity currents with loss of mass, such as particle-driven gravity currents, are provided.

---

### 1. Introduction

An inertial gravity current is formed by fluid flowing along a boundary under the influence of gravity into another fluid of different density. The foremost part of this flow is a characteristic head which is deeper than the following flow and has a projecting nose a short distance above the ground, and a series of lobes and clefts which continually change shape. Behind the head the current flows as a shallow layer with relatively little mixing with the surrounding fluid. Most of the mixing between the current and the environment takes place at the head via these lobes and clefts and by Kelvin–Helmholtz billows at the rear of the head. Numerous examples of gravity currents in the environment and laboratory are described by Simpson (1997).

There are many important situations where gravity currents flow over porous media with a consequent loss of mass from the current. One example concerns the motion of internal waves impinging on the continental shelf where the surge of the wave as it breaks takes the form of a gravity current which can interact with the sediment on the shelf (Thorpe 1966; Wallace & Wilkinson 1988; Boczar-Karakiewicz, Bona & Pelchat 1991). The storage of toxic or flammable liquids and dense gases in containers surrounded by gravel beds constitutes another example. The actual situation is complicated by evaporation into or chemical reaction with the ambient fluid, by the form of the underlying surface (see Britter 1989 and references

<sup>†</sup> Permanent address: Instituto de Física Arroyo Seco, Facultad de Ciencias Exactas, Universidad Nacional del Centro de la Provincia de Buenos Aires, Pinto 399, 7000 Tandil, Argentina.

therein) and the high density ratios between the released fluid and the surroundings (Grobelauber, Fannelop & Britter 1993). In the event of a spill of such a fluid the material may flow across the gravel as a gravity current.† The most important practical aspects are the determination of the mass absorbed by the porous media, and the maximum distance the current travels before stopping (Fannelop & Zumsteg 1986). Knowledge of this length would be very useful for safety calculations concerning possible eventual fire or toxic hazards.

A common procedure for generating gravity currents in the laboratory is the sudden removal of a vertical barrier separating two fluids of different densities in a channel of rectangular cross-section and solid bottom (lock-exchange experiments) (Keulegan 1957; Simpson & Britter 1979; Huppert & Simpson 1980; Rottman & Simpson 1983; and Hacker, Linden & Dalziel 1996). Most experiments have dealt with the intrusion of a saline solution of density  $\rho_s$  into an expanse of fresh water of slightly lower density  $\rho$ , and Reynolds numbers large enough for viscous effects to be negligible. From these experiments it is well-known that the gravity current so produced passes through two distinct phases. In the first stage, or *slumping phase*, the head of the current maintains nearly constant depth and travels at constant velocity  $u_f$  given by

$$u_f = C(\phi_0) u_0 \quad (1.1)$$

where  $0.5 \leq C(\phi_0) \leq 0.7$  (Rottman & Simpson 1983),  $\phi_0 = h_0/H$ ,  $h_0$  is the height of the dense fluid before release,  $H$  is the depth of the surrounding fluid,  $u_0 = (g'h_0)^{1/2}$ , and  $g' = g(\rho_s - \rho)/\rho$  is the reduced acceleration due to gravity. This stage, for which the initial conditions are important, ends when a bore coming from the rear wall overtakes the front at a certain distance from the gate of the order of several lock lengths  $x_0$  depending upon  $\phi_0$  (Rottman & Simpson 1983; Simpson 1997). Starting from this moment the current decelerates and decreases in depth, tending to a self-similar regime with the motion determined by a balance between the inertia of the gravity current and the driving buoyancy force, and by the boundary conditions at the front (Fay 1969; Hoult 1972; Huppert & Simpson 1980; Grundy & Rottman 1985). The horizontal length  $x_f$  of the gravity current for this second phase is

$$x_f = \eta(g'A_0)^{1/3} t^{2/3}, \quad (1.2)$$

where  $\eta = \eta(\phi_0) \approx 1.35$  for  $\phi_0 = 1$  (Huppert & Simpson 1980; Grundy & Rottman 1985; Simpson 1997),  $A_0 = x_0 h_0$  is the volume of the dense fluid per unit width of the channel, and  $t$  is the time measured from release. This type of behaviour is exhibited by similarity solutions of the depth-averaged shallow-water equations derived by Fannelop & Waldman (1972) and Hoult (1972), and may be extended to axisymmetric flows in which case  $x_f$  is proportional to  $t^{1/2}$  instead  $t^{2/3}$  (Fay 1969; Huppert & Simpson 1980). Grundy & Rottman (1985) showed that these similarity solutions are stable to linear perturbations and that they are indeed the large-time limit of the solution of the initial-value problem.

If the Reynolds number of the gravity current drops sufficiently, another phase occurs in which viscous forces are important. Assuming a balance between buoyancy and viscous forces in a current of fixed volume, Huppert (1982) (see also Marino *et al.* 1996), derived and experimentally corroborated a self-similar solution using the

† The name given to the flow usually depends upon the situation. For example, Britter (1989) denotes the spreading of a dense gas into ambient air as a plume or puff according to whether the release is continuous or instantaneous, respectively. Here we prefer to name it a gravity current due to its physical properties instead of the kind of release (and according to Simpson 1997).

lubrication approximation theory which gives the front position as proportional to  $t^{1/5}$  and  $t^{1/8}$  for planar and axial symmetry, respectively. By using the power laws corresponding to the inertial and viscous self-similar regimes, Huppert & Simpson (1980) and Grundy & Rottman (1985) determined the critical values of the time and the front position associated with the transition from one regime to another.

There are many analytical and numerical studies of gravity currents with increasing mass, which may be related to the problem studied in this paper in which mass is lost through the base of the current. Maxworthy (1983) performed a series of experiments in which he pumped salt water at a variable inflow from a source at the origin of coordinates, so that the volume of the denser fluid in the tank was proportional to  $t^\alpha$  ( $1.5 \leq \alpha \leq 3$ ) and he observed that the length of the plane current eventually became proportional to  $t^{(\alpha+2)/3}$ . Grundy & Rottman (1986) found that under certain conditions unique similarity solutions exist for the plane flow for all  $\alpha \geq 0$ , but that no similarity solutions exist in the axisymmetric case that satisfy the boundary condition at the axis of symmetry, except when  $\alpha = 0$ . Gratton & Vigo (1994) reinvestigated in detail all possible self-similar solutions generated in the previous conditions for plane gravity currents by means of the phase-plane technique. They showed that there is an infinite number of ways to set up a source which gives an inflow  $t^\alpha$  and the source must be characterized by another parameter such as the Froude number near by. Then, new continuous and discontinuous self-similar solutions with and without hydraulic jumps are found for large ranges of Froude number for the current and near the source. However, these studies have not been extended to constant or variable withdrawal corresponding to, for example, the loss of mass from a gravity current over a porous substrate.

An important case of gravity currents with variable mass is that of the *sedimentary* gravity currents (Middleton 1993; Simpson 1997). *Turbidity currents* are one type of sediment gravity flow in which the excess density derives from the presence of particles dispersed throughout the flow which are maintained in suspension by turbulence generated by the mean flow. They have strong similarities with gravity currents over porous media, in particular if they have negligible entrainment of the sediment from the bed. Since the presence of the particles is the cause of the motion, these currents also are called *particle-driven* gravity currents. Bonnecaze, Huppert & Lister (1993) have described them by means of shallow-water equations, obtaining a numerical solution which compares very well with their experimental results and provides a good idea of the flow developed. Dade & Huppert (1995) proposed an integral model whose analytical predictions agree very well with the laboratory observations and the numerical results of Bonnecaze *et al.* (1993). They obtained the scaling law for the front evolution which has two time scales, as is the case in the present work. The results concerning sedimentary gravity currents are compared throughout the paper, and are finally summarized in §4.

Only a few previous experiments concerning gravity currents running over porous media have been reported to our knowledge. Fannelop & Zumsteg (1986) investigated the spreading of heavy gases over ground with cavities. In their laboratory experiments the cavities are simply the open regions between narrowly spaced ribs on the floor of a two-dimensional channel. A simple integral model is presented but, unfortunately, no relevant experimental data are provided for comparison. Lionet & Quoy (1995, see also Simpson 1997, pp. 182–184) carried out preliminary laboratory experiments by using an experimental set-up analogous to ours. They produced gravity currents in a rectangular-cross-section tank by the release of salt water into fresh water over a porous surface modelled by two metallic grids put on of top each other. A

lock-exchange system with a partial gate opening was used. They measured the front position as a function of time and showed it is a parabolic decreasing function of time, which is also obtained by the model introduced in §4. By using different hypotheses for the behaviour of the porous substrate and for the height distribution, several simple integral models were proposed and numerically solved in order to explain the front evolution.

The aim of the present work is to extend the study of inertial gravity currents to the case in which the bottom is a horizontal porous surface. In our experiments, the gravity currents are produced by the instantaneous release of a fixed volume of salt water into fresh water in a rectangular-cross-section tank. The porous substrate is formed by thin metallic grids placed a given distance above the solid bottom, thus separating the tank into two parts. Dense liquid is released over the porous substrate, developing a gravity current at the same time as it partially flows downwards. The experimental set-up minimizes the effects of the flow upwards through the grid and an eventual interaction with the gravity current, as the bottom part of the tank is deep. The arrangement allows us to determine how, where and when salt water penetrates the porous surface, and leads to a simplified theoretical treatment of the problem.

An image-processing system, *DigImage* (Dalziel 1993, 1995; Hacker *et al.* 1996) is used for obtaining the density distribution of the gravity current and the mass which is below the porous substrate. It enables the detailed internal structure of the current to be measured, and this provides physical insight into the interaction of the gravity current with the porous substrate.

As this paper is mainly based on experimental results, we describe first the experimental set-up and the measurement techniques used, in order to clarify the details of the physical phenomenon studied (§2). Then we give a qualitative description of our observations in §3, in particular the position of the foremost part of the current (the *front*) as a function of time for two porous bottoms with different permeability, the evolution of the Reynolds number at the head, a typical sequence of iso-density contours and the fraction of the total mass present above the porous surface as function of time. This allows us to show the exponential decrease of  $M(t)$ , the ratio of the salt water mass at time  $t$  above the porous surface to the total mass released, and find the decay time  $\tau$  which is essential to understand the whole behaviour of the gravity current. Section 4 is devoted to discussing the results and a simple model is introduced which allows for the loss of mass from the current in calculating the velocity and depth. This model indicates that the height profile and the front position evolution play secondary roles in determining  $M(t)$ . The results obtained are contrasted with those of particle-driven gravity currents. Finally, in §5 a brief summary and the conclusions are given.

## 2. The experiments

Gravity currents were generated in a tank (230 cm long, 15.2 cm wide and 60 cm deep) with transparent Perspex sidewalls by means of the lock-exchange system depicted in figure 1. On one side of the tank, fluorescent strip lights and a light-diffusing screen provided nearly uniform back-lighting. A video camera was placed at a fixed position far away (300 cm) from the tank. Each experiment was recorded on a SVHS videotape. The porous substrate was a 0.05 cm thick metallic grid with 0.07 cm diameter holes and 0.2 porosity, located 15.5 cm above the bottom of the tank extending from the solid bottom of the lock to near the opposite end of the tank. In one series of experiments, two of these grids were employed together with their holes

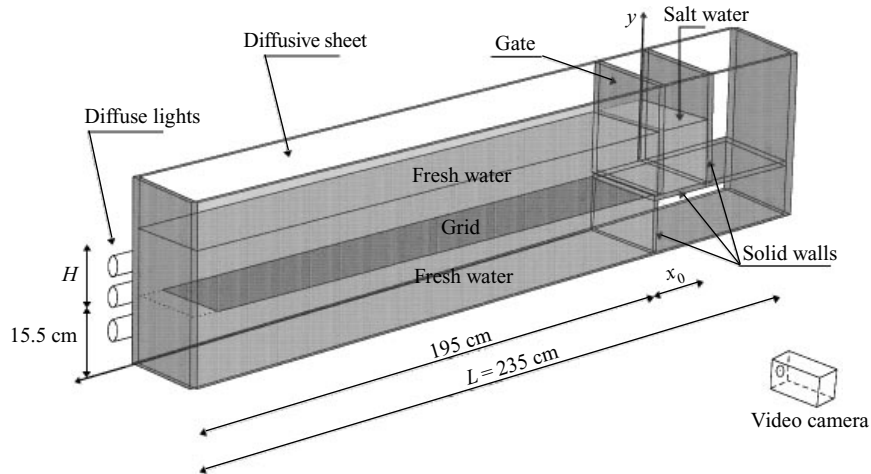


FIGURE 1. Schematic diagram of the experimental set-up.

partially superposed in order to decrease the permeability of the porous surface. We found that permeability was not completely uniform throughout the substrate and the superposition of the grids could not be regulated exactly. However, the results of these experiments seem to be insensitive to these problems, and they are also reported in the next section by using an average value of permeability.

The lock was formed using two vertical plates: an endwall which remains fixed during each experiment, and a gate located at a distance  $x_0$  from it, where the porous surface starts (see figure 1). The tank was filled with fresh water to a depth  $H$  above the porous surface. In all cases a full-depth lock was used with  $h_0 = H = 20$  cm. A known quantity of salt was dissolved into the water of the lock to create a density difference  $\rho_s - \rho$ . Also, a previously measured quantity of dye was added to the salt water to provide flow visualization. The experiment starts when the gate is quickly removed, leaving the dense fluid to flow out along the porous surface. Salt water also flows downwards through the grid to the lower part of the tank and, as a consequence, some fresh water needs to flow upwards. In order to limit the interaction between the flow of fresh water through the porous substrate and the gravity current, a space was left between the grid and the endwall of the tank (as figure 1 shows). In this way we find that the most of the fresh water goes upwards through this unrestricted opening and the residual flow through the grid does not affect the dynamics of the gravity currents throughout the substrate.

A series of equidistant 5 cm lines on the sidewall of the tank facing the video camera enabled us to determine the position of the front  $x_f$  (measured from the endwall of the lock) as function of time. The fixed position of the video camera introduces a small error by parallax which is taken into account in the reported values of  $x_f(t)$ .

A set of 46 experiments in three series were carried out in which the gravity current runs on a solid bottom, a double grid and a simple grid, respectively, by varying the initial lock lengths  $x_0$  (5, 10, 15, 23 and 40 cm) and  $g'$  (9.8, 49 and 98 cm s<sup>-2</sup> corresponding to a relative difference of density of about 1%, 5% and 10%).

By analysing digitized images taken from the video-tape, measurements of density distribution were made using the image processing software *DigImage* developed at DAMTP. The light attenuation of the back-lighting due to the dye present in the salt water allows the cross-current averaged dye concentration to be measured from

which the cross-current average density may be inferred. By integrating the density distribution we calculated the salt water mass present above and below the porous surface, and the total amount of salt (used to check data). The relative quantities of salt water mass are found to be more precise than absolute amounts due to partially cancelled errors, and they are reported below.

### 3. Results

We observe that gravity currents over the porous substrates studied have a head slightly deeper than the rest of the current with a poorly defined length and whose foremost point is raised above the surface. The typical instabilities of the inertial gravity currents are also present, which generate lobes and clefts at the front, and a mixing region of billows behind the head and above the tail of the current.

Figure 2 presents the evolution of the front positions of gravity currents running over the solid bottom in order to compare them with those generated over the porous bottoms under the same initial and boundary conditions, and to test the experimental system. As usual, the front position is scaled by the initial lock length  $x_0$  and the time after release is scaled with the characteristic time of the slumping phase  $t_c = x_0/(g'h_0)^{1/2}$ . Thus,  $g'$  and  $A_0$  are included into the space and time scales in the self-similar stage also. In fact, (1.2) may be written as

$$\frac{x_f}{x_0} = \eta \left( \frac{t}{t_c} \right)^{2/3}. \quad (3.1)$$

The experimental points show some systematic departures owing to the influence of the initial conditions and instabilities, but the behaviour for all cases is essentially the same. As expected, we observe the initial slumping phase (dashed-dot line with slope 1), and later the self-similar phase (dashed line with slope  $\frac{2}{3}$ ) develops after approximately 10 lock lengths. Figure 2 shows no evidence of the presence of a viscous phase because the critical values (time and front position) corresponding to the viscous transition have not yet been reached.

Figure 3 presents the experimental results from gravity currents running over the low-permeability substrate formed by two overlapping grids. The same two power laws shown in figure 2 are also given for comparison. At first sight, the analogy between the results reported in figures 2 and 3 suggests that the front motion is little modified by this porous substrate. The solid lines are calculated by the model introduced in §4, and they will be discussed in that section.

Greater deviations occur when gravity currents are developing over a substrate with higher permeability, formed by the simple grid, as figure 4 shows for some typical cases. During the slumping phase the front velocity is clearly non-constant and the second self-similar stage is not present. Note the striking variety of behaviour. The slowing down of the front position is related to the greatest values of the lock length and of the reduced gravity used. This behaviour resembles that obtained from particle-driven gravity flows where the length of the current increases more slowly as  $g'$  increases, for increasing particle size or initial masses of sediment released (Bonnecaze *et al.* 1993).

In order to discard viscous effects as responsible for this new phase, we calculate the Reynolds number at the current head

$$Re = u_f h_n / \nu, \quad (3.2)$$

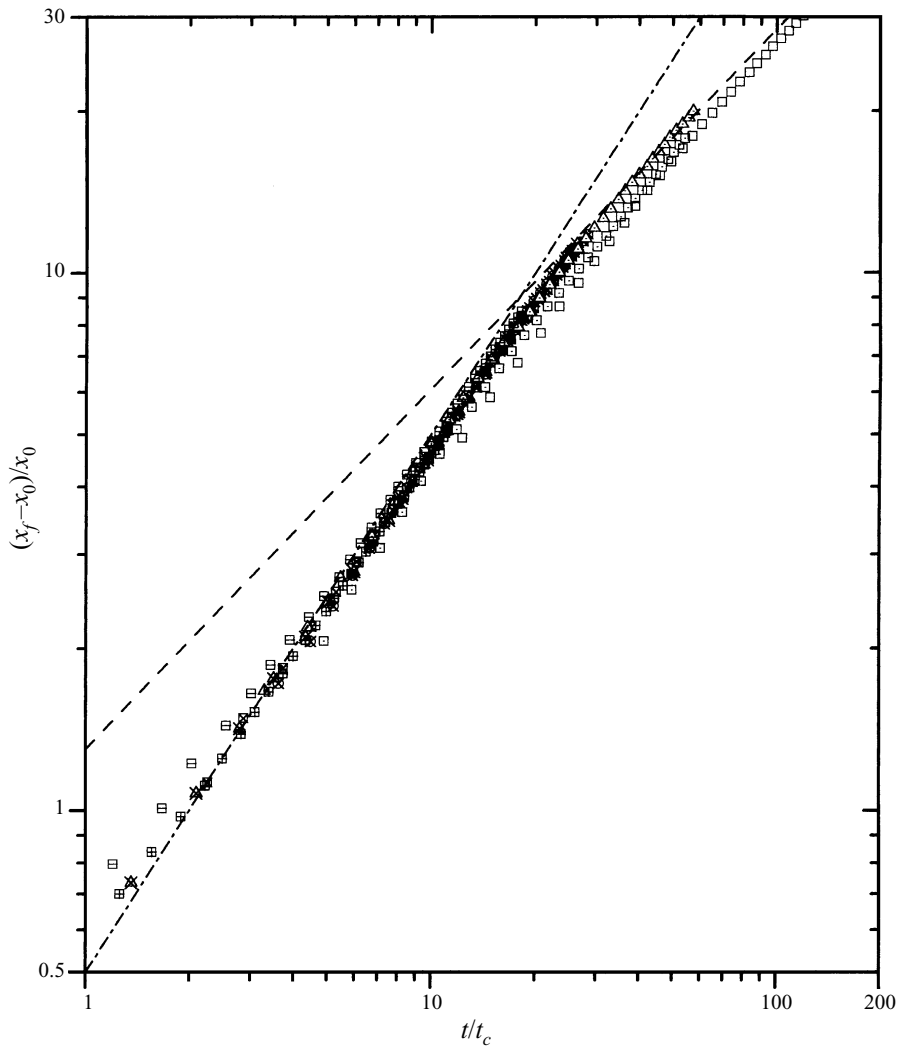


FIGURE 2. Front positions in units of the lock length  $x_0$  as a function of time from release, for experiments with different  $x_0$  and  $g'$  carried out on a solid bottom. The two phases are well represented by  $(x_f - x_0)/x_0 = 0.5t/t_c$  (dashed-dot line), and  $(x_f - x_0)/x_0 = 1.35(t/t_c)^{2/3}$  (dashed line). The symbols correspond to:  $g' = 9.8 \text{ cm s}^{-2}$  (circles),  $49 \text{ cm s}^{-2}$  (squares) and  $98 \text{ cm s}^{-2}$  (triangles), for  $x_0 \approx 5 \text{ cm}$  (open symbols),  $10 \text{ cm}$  (dotted symbols),  $15 \text{ cm}$  (symbols with  $\times$ ),  $23 \text{ cm}$  (symbols with  $-$ ), and  $37 \text{ cm}$  (symbols with  $+$ ).

where  $u_f = dx_f/dt$ ,  $h_h$  is the thickness of the current head, and  $\nu$  is the kinematic viscosity.

In our experiments the Froude number  $F$  at the head given by

$$F = u_f/(g'h_h)^{1/2} \quad (3.3)$$

is almost constant and approximately equal to unity throughout the range of the parameters used. This agrees with the results of gravity currents running over solid substrates whose characteristic parameters have analogous values (Benjamin 1968; Britter & Simpson 1978; Simpson & Britter 1979; Huppert & Simpson 1980). Equation (3.3) may be also obtained by simple local energy or momentum balance (see,

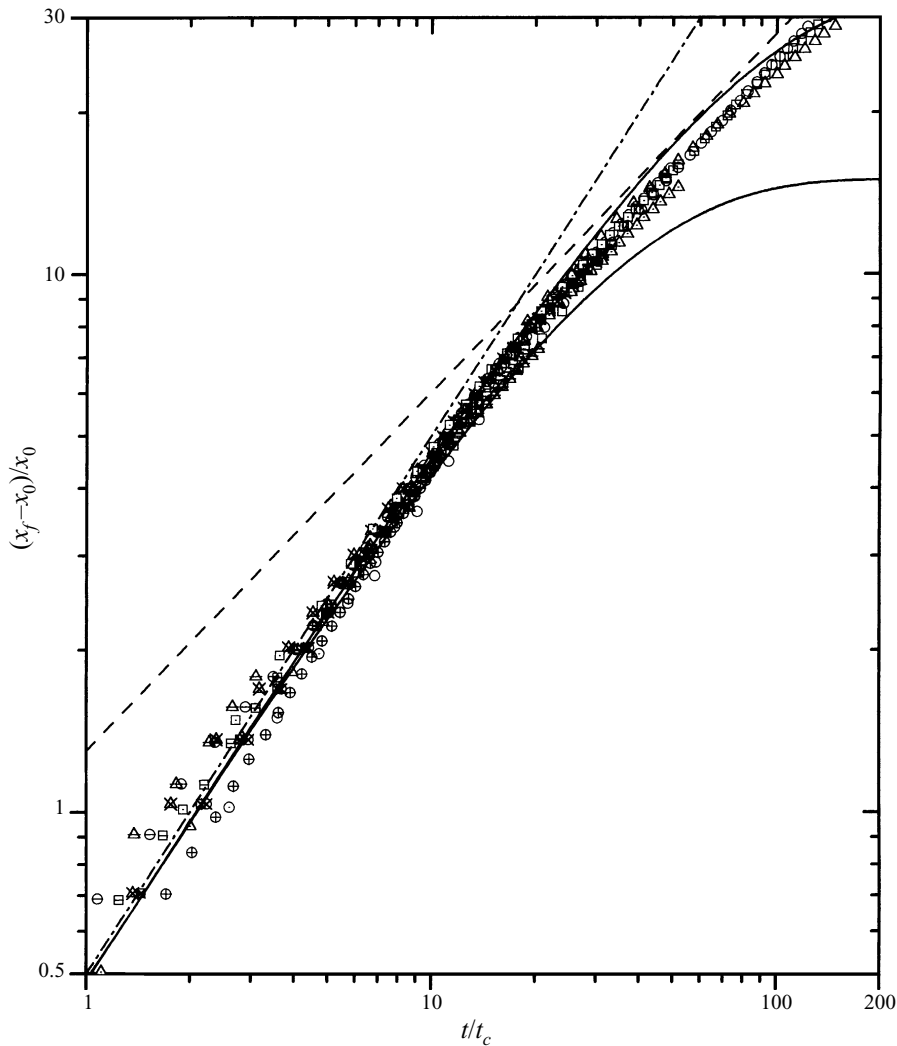


FIGURE 3. Evolution of the non-dimensional front position for gravity currents running on the low-permeability substrate formed by two superposed metallic grids. The solid lines represent the limit curves given by (4.10) for the parameters of the experiments. The symbols correspond to the same values of the parameters  $x_0$  and  $g'$  given in the caption of figure 2.

for instance, Simpson 1997 and Grobelbauer *et al.* 1993). Since the values of  $F$  show scatter because of the uncertainties in our measurements of  $u_f$ ,  $g'$  and  $h_h$ , we prefer to calculate  $h_h$  in (3.2) by means of (3.3).

Figure 5(a–c) shows the evolution of  $Re$  in the experiments carried out over a single grid. In spite of the spread of results obtained in figure 4, the Reynolds number as a function of time collapses onto three different curves according to the value of  $g'$ . The evolution of  $Re$  is also smoother than the corresponding evolution of gravity currents running over a solid bottom or particle-driven gravity currents (Bonnecaze *et al.* 1993). These Reynolds numbers are much greater than the critical value  $Re_* \approx 50$  (see Appendix), suggesting that the front evolution is determined by the effects of the decrease of mass of the current rather than by viscous effects. Eventually they reach

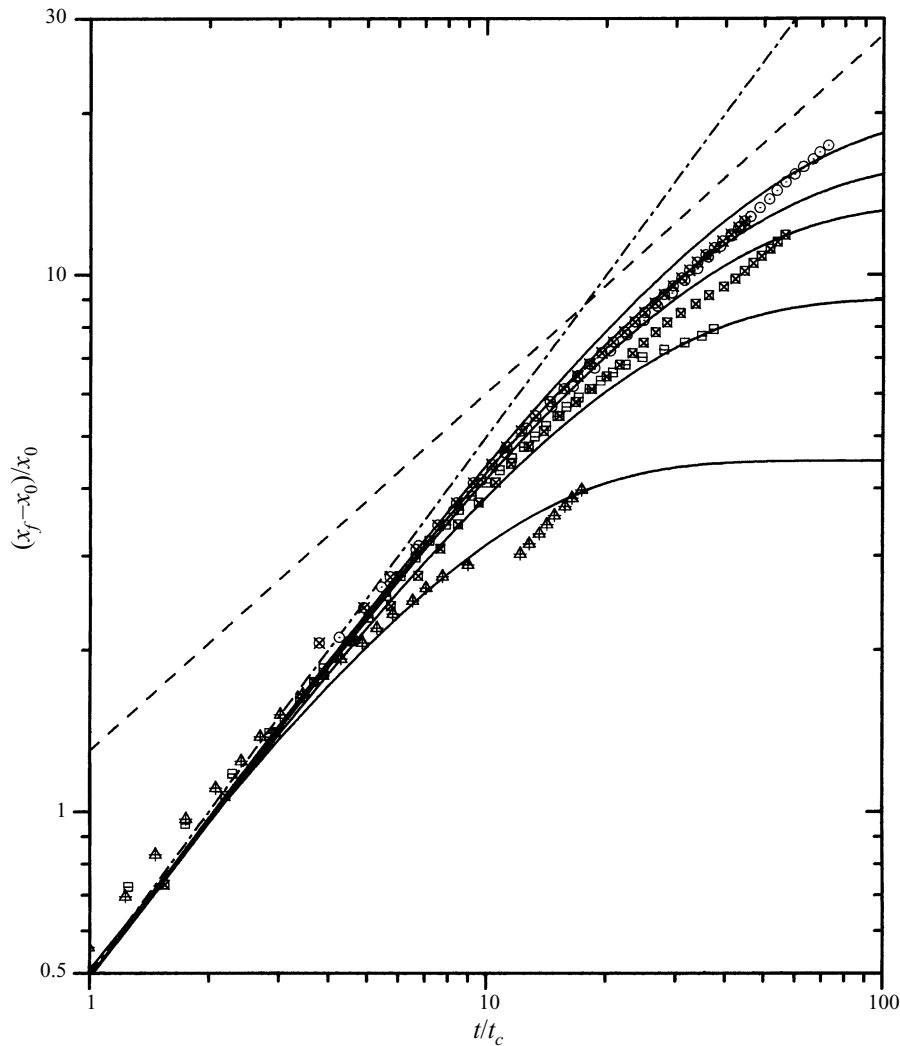


FIGURE 4. Evolution of the non-dimensional front position for some gravity currents running on the higher permeability substrate constituted by a single metallic grid. The solid lines are given by (4.10) for each experiment reported. The symbols correspond to the same values of the parameters  $x_0$  and  $g'$  given in figure 2.

the critical value, but more experimental information is required to investigate the viscous regime (i.e.  $Re \lesssim 50$ ).

Contours for densities corresponding to  $\rho_\varepsilon = \rho + \varepsilon(\rho_s - \rho)$ , with  $\varepsilon = 0.05, 0.33$  and  $0.66$  (short-dashed, long-dashed and solid lines, respectively), for a typical gravity current over the simple grid are shown in figure 6. These contours may be thought as corresponding to extreme ( $\varepsilon = 0.05$ ), moderate ( $\varepsilon = 0.33$ ) and slight ( $\varepsilon = 0.66$ ) mixing with the surrounding fluid. In figure 6(a) we observe the contours immediately after the gate is removed. Inside the lock zone and over a small part of the grid, most of the salt water is still highly concentrated ( $\varepsilon \geq 0.66$ ) displaying the beginning of a gravity current. Inside the lock zone, there is mixed fluid generated during the removal of the gate. At this stage a small quantity of salt water is detected under the grid near the gate. The fluid flowing down through the grid becomes important, taking a

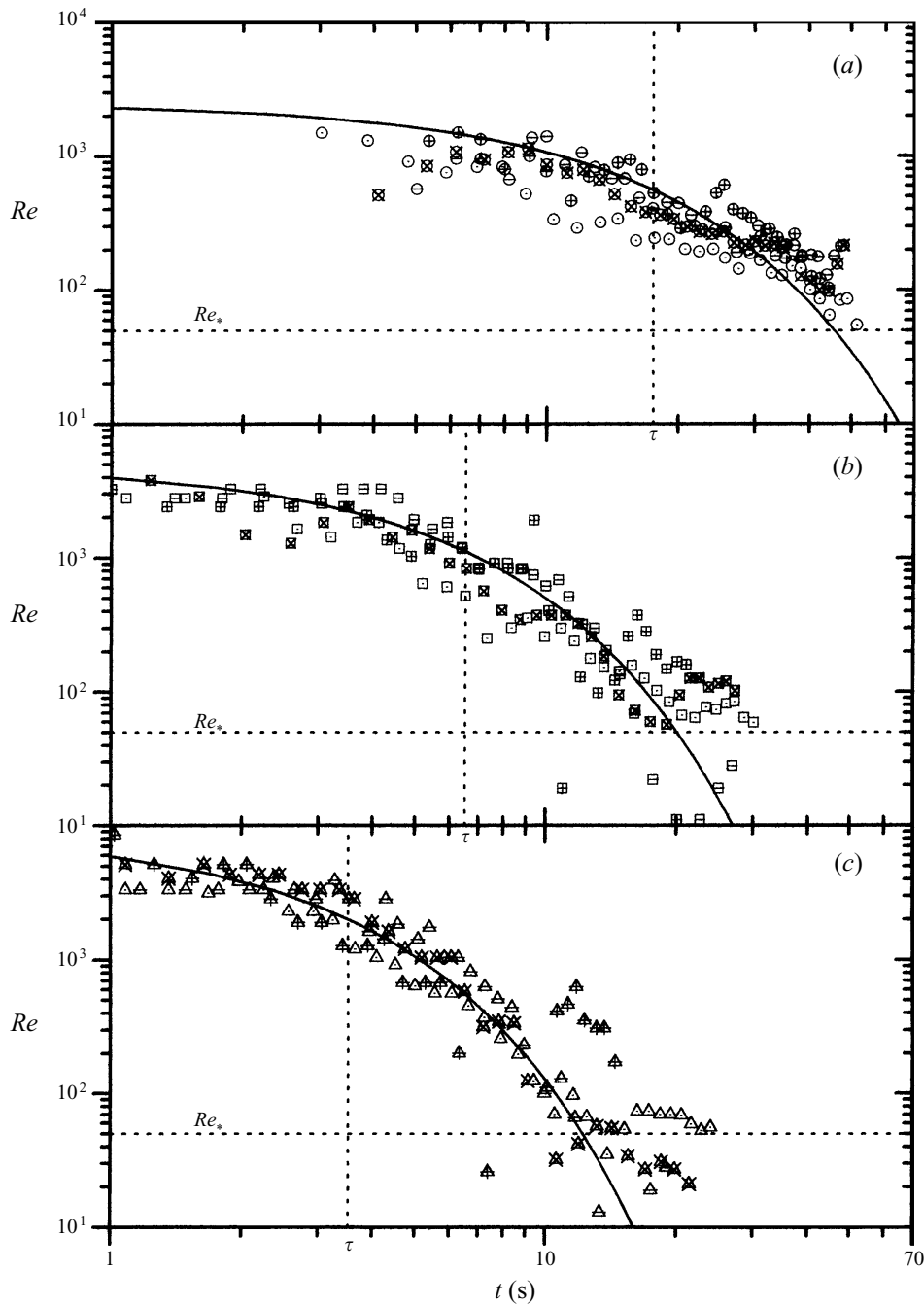


FIGURE 5. Log-log variation of  $Re$  with time for: (a)  $g' = 9.8 \text{ cm s}^{-2}$ , (b)  $g' = 49 \text{ cm s}^{-2}$ , and (c)  $g' = 98 \text{ cm s}^{-2}$ , when the porous substrate is a single grid. The evolution of  $Re$  described by the solid lines is given by (4.9) for the corresponding parameters.

significant part of the salt water under the grid, while the remaining volume develops the foremost part of a gravity current (figure 6*b*). The upper current goes on ahead while losing more mass (figure 6*c*) and its foremost part acquires a density value much smaller than the initial one (figure 6*d*). Simultaneously the front decelerates (as

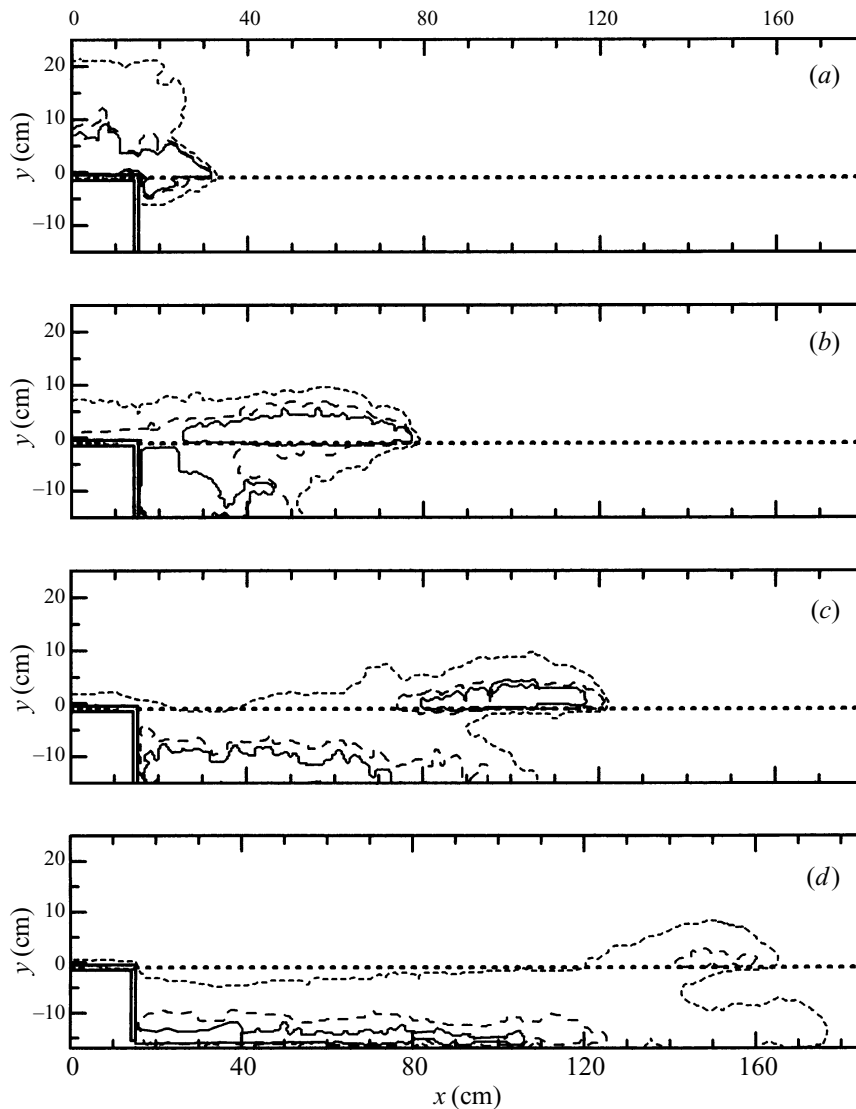


FIGURE 6. Evolution of the iso-density contours obtained for the experiment with  $x_0 = 15.2$  cm and  $g' = 50.47$  cm s $^{-2}$  at (a)  $t = 1.24$ , (b) 5.08, (c) 10.36, (d) 18.70 s for which  $Re = 3800$ , 1500, 400 and 60, respectively.

seen in figures 4 and 5) until almost all the salt water is below the grid. In figures 6(c) and 6(d) we note that the tail of the current is vanishing leaving only the head. Observe the well-developed nose at the front of the gravity current in spite of the loss of mass from the current. Figure 6 suggests that most of the dense liquid is lost through the porous substrate in the zone near the lock and at the early times of the gravity current evolution.

The iso-density contours above the porous surface shown in figure 6(a–d) may be qualitatively compared to those reported by Hacker *et al.* (1996). They describe the density structure of gravity currents and present some results for gravity currents over rigid bottoms generated by the lock-exchange technique in a rectangular channel.

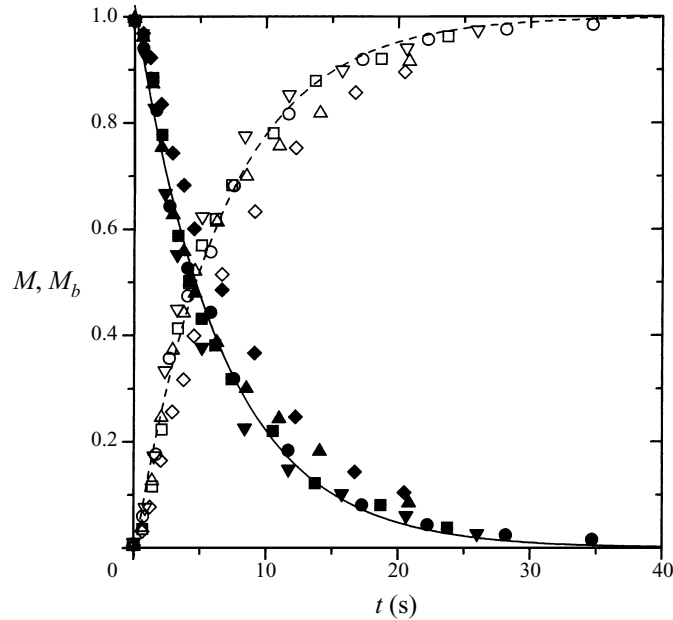


FIGURE 7. Evolution of non-dimensional salt water masses  $M(t)$  (solid symbols) and  $M_b(t)$  (open symbols), over and below the porous substrate, respectively, for a simple grid,  $g' = 49 \text{ cm s}^{-2}$  and  $x_0 = 6.2 \text{ cm}$  ( $\bullet$ ),  $x_0 = 10.0 \text{ cm}$  ( $\blacktriangledown$ ),  $x_0 = 15.2 \text{ cm}$  ( $\blacksquare$ ),  $x_0 = 22.8 \text{ cm}$  ( $\blacktriangle$ ),  $x_0 = 37.4 \text{ cm}$  ( $\blacklozenge$ ). The decay time given by the best-fit exponential function (solid line) for the first four cases is  $\tau = 6.53 \text{ s}$ .

Figure 6(a) shows a stronger decrease of the fluid height at the endwall because the porous substrate provides an extra exit for the dense liquid of the lock. The typical shallow layer of dense liquid behind the head of a gravity current over rigid bottom is absent in figures 6(b) and 6(c), where highly mixed fluid remains. The head structure depicted in figure 6(b,c), however, resembles quite closely that obtained for gravity currents over solid bottoms. On the other hand, figure 6(d) shows no tail at all and also the density of the head has been reduced appreciably in contrast to the currents reported by Hacker *et al.* (1996), but similar to the flow corresponding to the latter stages of particle-driven gravity currents. From this comparison, it is clear that the porous substrate influences the motion of the current by extracting fluid directly from the head, and also from the dense layer behind it.

Figure 7 shows  $M(t)$  (and  $M_b(t)$ ) defined as the ratio between the salt water mass at time  $t$  located above (and below) the porous surface per unit width and the total salt water mass released for a single value of  $g'$  and a range of lock lengths. Throughout the range of volumes covered ( $1.67\text{--}12.16 \text{ cm}^3$ ), we see that  $M(t)$  coincides pretty well for the different cases. A small deviation from the general behaviour is observed for the latest times for the largest volume released ( $\blacklozenge$ ), probably because the salt water volume which passed through the grid partially saturates the space below the grid and modifies the flow there. The evolution of  $M(t)$  is well fitted by an exponential law (solid line) with a time of decay  $\tau = 6.53 \text{ s}$  which is of the order of the time these experiments last. Figure 7 indicates that the flow through the porous bottom is independent of the volume released, provided there is no saturation under the grid. It also suggests that the loss of mass of the gravity current does not depend on the depth of the overlying layer of ambient fluid, in contrast to particle-driven gravity currents.

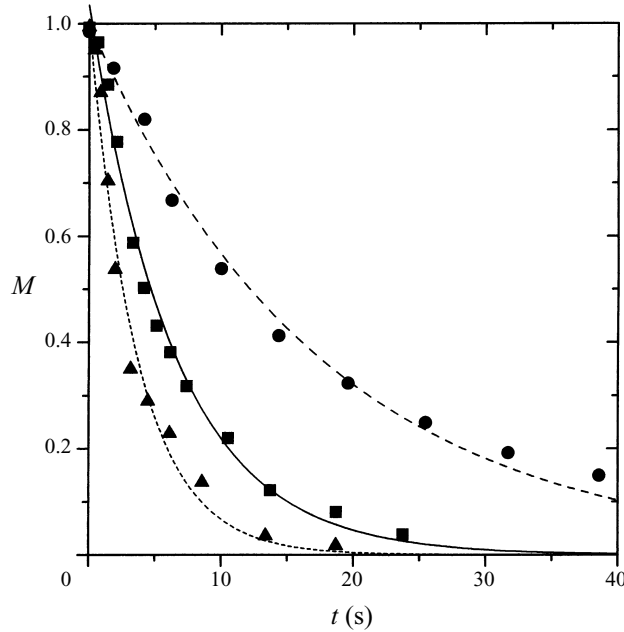


FIGURE 8. Non-dimensional salt-water mass  $M(t)$  for some experiments performed using a single grid as porous surface. The symbols correspond to:  $x_0 \approx 15$  cm and  $g' = 9.8$  cm s $^{-2}$  (●), 49 cm s $^{-2}$  (■), and 98 cm s $^{-2}$  (▲). The best-fit exponential functions have decay times  $\tau = 17.57$ , 6.53 s and 3.52 s, respectively.

The same behaviour is observed in the double-grid experiments, but the constant of decay is slightly greater ( $\tau = 8.4$  s), corresponding to a smaller permeability.

Figure 8 shows  $M$  as function of time for three different values of  $g'$  for a fixed volume released over a single grid. The evolution of  $M$  for these cases are well fitted again by exponential laws, with characteristic time of decay proportional to  $g'^{-0.8}$ . Therefore, the dynamic similarity for gravity currents with different  $g'$  is broken when they run over porous media. An explanation of all these results is contained in the model introduced in the next section.

#### 4. Discussion

The experimental results suggest that gravity currents running over porous surfaces have, to a first approximation, an exponential decrease of the bulk mass. This distinctive feature may be understood by means of the following heuristic model. Consider a homogeneous current of density  $\rho_s$ , and neglect any mixing between the current and its surroundings. The Reynolds number for the flow through porous media is defined as  $Re' = Ql/v$ , where  $l$  is some length dimension of the porous matrix (the hole diameter, for example) and  $Q$  is the discharge per unit area. For all practical cases, the vertical flow through the porous substrate may be described by Darcy's law (Bear 1972; Duillen 1979) provided that  $Re'$  does not exceed a value about 10 which is not exceeded in our cases. Therefore, the vertical component  $v$  of the flow velocity at any horizontal position  $x$  is proportional to the pressure gradient  $\nabla p$  when applied on the  $d$ -thickness grid. Thus,

$$v(x, t) = \frac{k}{v} |\nabla p| \approx \frac{kg'h(x, t)}{vd} = \frac{h(x, t)}{\tau} \quad (4.1)$$

with

$$\tau = \frac{vd}{kg'}, \quad (4.2)$$

where  $k$  is the specific permeability,  $h(x, t)$  is the height of the dense fluid over the porous substrate and  $\nabla p$  is assumed to be hydrostatic, which is the case when the length of the current is much larger than its depth and vertical accelerations can be neglected. By using (4.1), the volume  $Q(t)$  per unit time and width lost by the gravity current due to the presence of a porous surface is given by

$$Q(t) = \int_{x_0}^{x_f} v(x, t) dx \approx \int_0^{x_f(t)} v(x, t) dx = A_0 \frac{A(t)}{\tau}, \quad (4.3)$$

with

$$A(t) = \frac{\int_0^{x_f} h(x, t) dx}{A_0}. \quad (4.4)$$

In (4.3) we are supposing that the flux through the bottom of the lock ( $0 \leq x \leq x_0$ ) is negligible even if it were porous. This assumption is valid starting from a short time after the beginning of the experiments, since the liquid height in the lock is strongly reduced by the bore coming from the head, as explained in §1.

The conservation of mass imposes that

$$1 = A(t) + \frac{1}{A_0} \int_0^t Q(t') dt' \quad (4.5)$$

and solving it, we find that

$$A(t) = e^{-t/\tau}. \quad (4.6)$$

Note that in obtaining (4.3)–(4.6) no assumption about the evolution of the front position and the height profile  $h(x)$  is needed; that is, it does not matter if the whole volume is uniformly distributed throughout the gravity current or it is concentrated in a small region near the front. Therefore, under the hypothesis which allows us to obtain (4.1), the porous bottom introduces a characteristic time  $\tau$  (not only local but for the whole flow) unrelated to a particular stage of the gravity current evolution.

Equation (4.6) indicates that  $A(t)$  (and  $M(t)$  since we have assumed no mixing in the flow) follows an exponential law with the time of decay  $\tau$  inversely proportional to  $g'$  and independent of  $A_0$ . These analytical predictions agree well with experimental results foreseen from figures 7 and 8. An additional verification arises from the fact that the value of  $k \approx 1.5 \times 10^{-6} \text{ cm}^2$  obtained from (4.2) using the experimental values of  $\tau$  is in agreement with the previous value estimated by Lionet & Quoy (1995), for the same grids, carrying out specifically designed experiments.

As described in §1, during the slumping phase of gravity currents running over a solid bottom, the current head moves with a quasi-constant velocity and the current height is also constant. At early times of the self-similar regime the height of the current head also does not vary much. Therefore, for the spreading over porous substrate we may suppose that the decrease of  $h_h$  is due to the loss of mass, and then  $dh_h/dt \approx -v$ . By using (1.1), (3.3) and (4.1), we obtain

$$h_h = \frac{C^2}{F^2} h_0 e^{-t/\tau}. \quad (4.7)$$

Note that the front condition (3.3) used is a momentum balance at the front.

Therefore, the drag force associated with the momentum loss due to the transfer of mass might be taken into account by adopting an effective value for  $F$ , as is usually done for the viscous drag, turbulent Reynolds stresses and entrainment drag in turbulent flow (see Huppert & Simpson 1980 and Fannelop & Zumsteg 1986). However, the change in the Froude number due to the grid appears to be negligible in our situation, because we do not detect any change in the measured Froude number when using a permeable bottom. More research and specific experiments are needed to clarify this point.

Thus, the front velocity is given by

$$u_f = Cu_0 e^{-t/2\tau} \quad (4.8)$$

and, thus, it can be supposed to be constant only if  $t \ll 2\tau$ .

Equation (4.8) also allows us to calculate the characteristic time  $\tau$  from the front position evolution, but only in an approximate way due to the scatter of the data which are sensitive to the initial conditions of the experiments. For example, the results shown in figure 4, for  $g' = 49 \text{ cm s}^{-2}$ , give  $4.5 \text{ s} < \tau < 9.8 \text{ s}$ , while the value  $\tau = 6.53 \text{ s}$  is obtained from figure 8.

From (4.7) and (4.8) the Reynolds number (3.2) can be written as

$$Re = Re_0 e^{-3t/2\tau}, \quad (4.9)$$

where  $Re_0 = Re(t = 0)$ . By plotting (4.9) for the corresponding parameters of figure 5 we obtain the solid lines which reproduce the main temporal dependence of  $Re$ .

On the other hand, by integrating (4.8) we find that

$$\frac{x_f}{x_0} = C \frac{2\tau}{t_c} [1 - e^{-(t_c/2\tau)t/t_c}]. \quad (4.10)$$

In contrast to the Reynolds number, the evolution of the front position depends on the two characteristic times of the problem:  $t_c$  and  $\tau$ , which are related to the initial conditions and the permeability of the porous substrates, respectively (even though both of them depend on  $g'$ ). Each experiment has particular values of these times, and only in a few cases do they combine to give the same value of  $t_c/2\tau$ . Thus, (4.10) suggests that the front position evolution for different experiments cannot collapse onto a single curve in a plot of  $x_f/x_0$  vs.  $t/t_c$ . For experiments carried out over the double grid, the respective evolution given by (4.10) corresponding to each experiment lies between the two limit curves plotted as solid lines in figure 3. Unfortunately, the finite size of the tank does not allow us to have front positions for more extended gravity currents in order to verify (4.10) for the lowest permeability substrate. However, a better comparison is possible for the highest permeability substrate. Figure 4 shows the agreement reached between the front position evolution for some experiments performed over a simple grid. Note that (4.10) suggests that the characteristic time and length scales are  $\tau$  and  $x_0 t_c / \tau = u_0 \tau = \nu d (h_0 / g')^{1/2} / k$ , respectively. Thus, the length scale represents the distance at which the dense fluid mass over the grid has decreased by a factor  $e^{-1}$ , and does not depend on  $x_0$ . The points shown in figure 4 are plotted in figure 9 with these scales, and the experimental points fall, as expected, on a single curve with relatively small dispersion near the curve given by (4.10).

As discussed in § 1, a decrease of the head height takes place as the length of the gravity current increases, which starts when the front has advanced about 10 lock lengths, or after a time  $t' = 20x_0/u_0$ . As we neglected this decrease,  $t'$  has to be greater

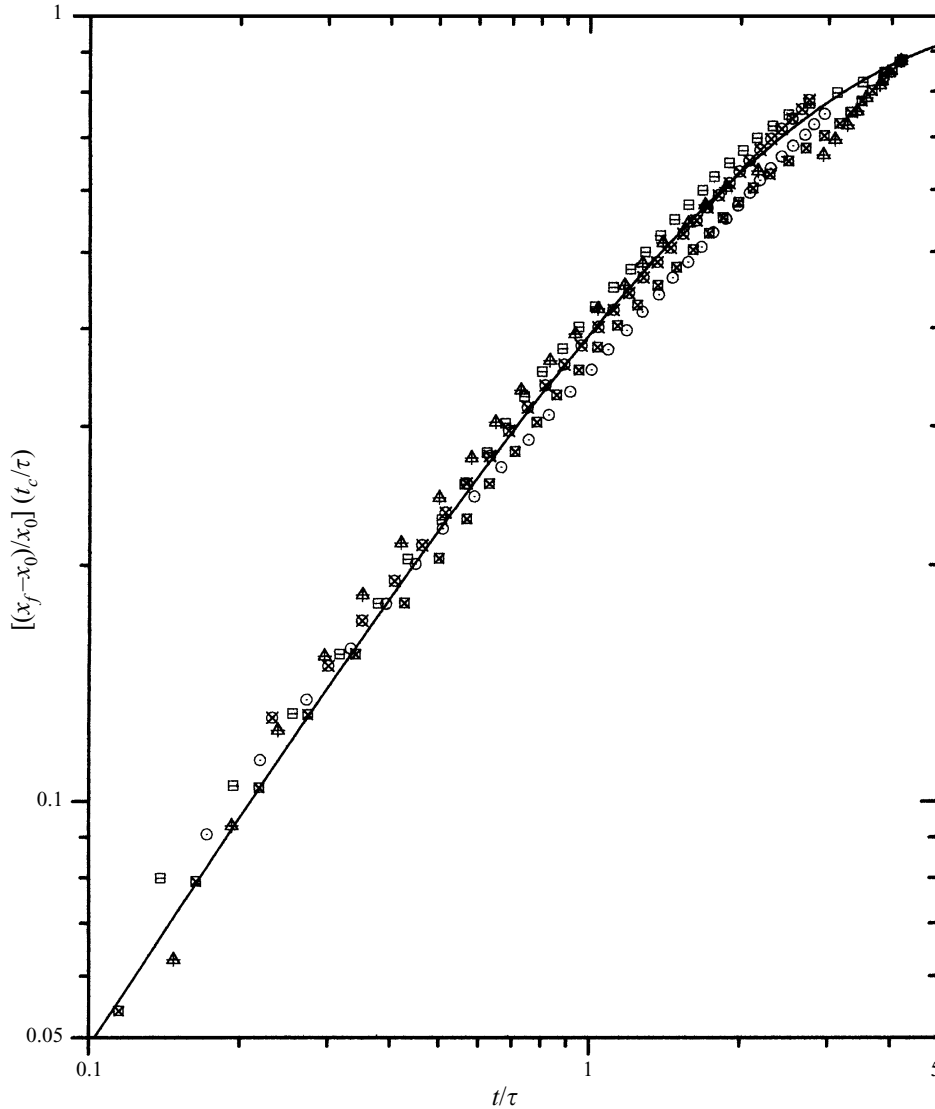


FIGURE 9. Evolution of the front position for the same currents reported in figure 4, now non-dimensionalized by the scales suggested by (4.10). The solid line is given by (4.10).

than  $2\tau$  for (4.7)–(4.10) to be valid. By using (4.2), we find that this condition requires

$$k \gtrsim \frac{vd}{10A_0} \frac{h_0^{3/2}}{g^{1/2}}. \quad (4.11)$$

That is, the evolution of the parameters which characterize the front are given by (4.7)–(4.10) for high-permeability bottoms. Most of the experiments described in §3 satisfy (4.11), with the exception of some experiments carried out over double grid for which  $k$  is slightly smaller than the value indicated by (4.11).

Now we are able to analyse our findings in the framework given by previous works related to turbidity gravity currents (or gravity surges) with no entrainment of the deposited particles. A useful comparison is possible by using predictions of the

theoretical model provided by Dade & Huppert (1995). Those authors proposed an integral model in which the current evolves through a series of equal-area rectangles between the leading and trailing boundaries, both dependent upon time, as the current propagates downstream over a solid bottom. It allows for the slow variation of  $g'$  due to settling of the particles. The problem has the time scale  $t_c$  given by the initial conditions and also another characteristic time scale  $t_s$  on which the effects of particle settling become important. The time scale  $t_s$  is proportional to  $(A_0^2/(g'_0 w_s^3))^{1/5}$  and  $(A_0^6/(h_0^2 g_1^3 w_s^7))^{1/13}$  for deep and shallow surroundings, respectively, where  $w_s$  is the average settling velocity of the particles in a monodisperse suspension. Both of those expressions for  $t_s$  are due to the fact that gravitational settling is strongly coupled with the velocity of the current, which depends on the fractional depth  $\phi_0 = h_0/H$ , as stated in §1.

Gravity currents over porous substrates also have two time scales:  $t_c$  and  $\tau = vd/kg'$ . As we said after (4.6), this second characteristic time scale does not seem to depend on the velocity of the current and the height profile. Therefore, the relationship between  $\tau$  and the initial spreading parameters is simpler than the corresponding time scale for gravity surges, with the only difference being between deep and shallow ambient fluid that comes from the variation of  $F$  with  $\phi$ .

Bonnecaze *et al.* (1993) described these currents by shallow-water equations derived from the usual hydraulic assumptions of vertically uniform flow and a hydrostatic pressure distribution within the current (assumptions also used in the present work). They give a description of the flow evolution which is quite different from the flow developed by the gravity currents over porous substrates due to the differences in the physical processes involved.

(a) In gravity surges the particles are maintained in the interstitial fluid due to, for example, turbulent mixing, which depends upon the initial parameters. Therefore, there may be a phase in which very few particles settle out of the current and the loss of mass of the current is negligible. This occurs especially when the currents have an initial height comparable to the depth of the surrounding fluid, due to the bore formed in the slumping phase.

(b) The instantaneous loss of mass in a given position depends upon the current height  $h$  through a quite different relationship. For example, when the sediment concentration is small in a turbidity gravity current, the rate of loss of particle concentration is inversely proportional to the depth of the current, while the flux through the porous substrate is proportional to  $h$ . Thus, the particles are preferentially removed from the rear of the current, due to the smaller height there.

(c) In gravity surges dense mass is lost through the particles settling out, but not the interstitial fluid which continues its motion even if it is particle-free.

The fact that the particles settle out more rapidly towards the rear of the current determines that the density and pressure gradient in the tail is reduced more strongly. Thus, the rearward fluid is not decelerated as much as the front region, and it accumulates behind the head, still relatively rich in particles. The thinning of the head region in the slumping regime is followed then by a gradual thickening, and finally a travelling shock is formed between the head and the tail of the current, which eventually reaches the front. This phenomenon appears to be completely absent in the gravity current over porous media, at least for uniform and constant porosity as studied here.

Thus, the complex interaction between the current and the settlement of particles determines a different Reynolds number evolution at the front. In particle-driven

gravity currents there is a drop in the  $Re$  values when the initial bore reaches the nose of the current, and they finally tend to an almost constant value determined by the particle-free interstitial current (Bonnecaze *et al.* 1993). This situation is completely different to that showed by figure 5. Here the loss of mass through the porous substrate smooths the curves, which are monotonically decreasing with time. Also, the asymptotic laws for  $t \gg t_c$  are completely different. For a gravity surge  $x_f$  is a power law of time, while (4.10) suggests an exponential relationship.

## 5. Concluding remarks

The influence of porous substrates on plane inertial gravity currents was investigated in experiments varying the lock length, the relative differences of densities between the fluids used, and by using two porous surfaces with different permeability. There are many effects to discuss in these experiments, but for clarity we restrict ourselves to the global behaviour of the gravity currents over porous media.

The results indicate that the mass of the dense fluid is lost through the porous substrate at an exponential rate with a decay time  $\tau$ , provided there is no saturation in the space below the porous surface. The loss of mass dominates the flow, and the value of  $\tau$  plays an important role in the evolution of the current. We find that the front velocity  $u_f$  and the head height  $h_h$  also decrease exponentially, and no self-similar regime is completely developed. The Reynolds number drops more quickly than in a gravity current running over a solid bottom, and so the viscous regime occurs earlier in the evolution of the current. All these results are described by a simple model without adjustable parameters, and which explains the exponential decrease of the total mass over the porous substrate. Simple local balances near the front are enough to obtain the front evolution observed experimentally. However, an integral model such as that presented by Dade & Huppert (1995) or numerical solutions of the shallow-water equation as given by Bonnecaze *et al.* (1993) for particle-driven gravity currents may also provide an alternative description for this problem when adapted to this situation.

The decrease of  $h_h$  (or  $u_f$ ) due to the increase of the length may be neglected under our conditions of strong loss of mass. We may also ignore the momentum equation in the whole flow and consider only local balances for the front movement. However, this is not the case for very low permeability of the substrate, where the loss of mass plays a secondary role in the evolution of gravity currents. Nonetheless, some of the results found, the model introduced or the ideas discussed above may help to understand those phenomena. They may also be useful in checking general numerical codes developed for engineering purposes.

The experimental results reported seem to be insensitive to the mixing between the current and the surrounding fluid. In our experiments the mixing changes when we vary the initial conditions (Hacker *et al.* 1996) and the Reynolds number (i.e. varying the lock lengths and reduced gravity values). However, the data may be understood without taking the mixing into account, probably because the flow through the porous substrate (see (4.3)) depends on  $g'$  and  $A_0$  through the product  $g'A_0$ . In fact, mixing reduces  $g'$  but increases  $A_0$ , and vice versa. Therefore no strong variation is expected in  $g'A_0$  for mixing and, as a consequence, in the evolution of gravity currents over porous substrate.

The results concerning the exponential loss of mass of an inertial gravity current over porous media might be directly extended to axial geometry. We point out, however, that the extension of the inertial regime is severely reduced in laboratory

experiments due to the early entrance of the viscous stage, because of the stronger decrease of the head velocity.

As shown in §4, the exponential decay of the salt water mass of the gravity current is obtained if the porous substrate is thin and provided there is no saturation under it. However, the present work may be considered as a first step towards a thorough study of gravity currents running over a deep porous media, where those conditions must be removed.

B.M.M. and L.P.T. acknowledge financial support from Consejo Nacional de Investigaciones Científicas y Técnicas de la República Argentina (CONICET) and Universidad Nacional del Centro de la Provincia de Buenos Aires, Argentina.

## Appendix

As stated in §1, several authors have estimated the time for the transition between the inertial and viscous self-similar regimes for a gravity current of a fixed volume running over a solid bottom. In experiments over porous substrates, however, we cannot assume that those regimes are self-similar because of the important influence of the loss of mass on the flow dynamics. In addition, in many cases we observe that the tail vanishes at a given time leaving the head only, as figures 6(c) and 6(d) show. Therefore, it is convenient to obtain a parameter associated with the transition to the viscous regime, as for instance the Reynolds number value at the current head, by using only values defined there.

In the initial stage, the front velocity  $u_f$  is related to the current head height  $h_h$  by the Froude number given by (3.3), while in the viscous regime the characteristic wheel-like shape of the head indicates that (Marino *et al.* 1996; Marino, Thomas & Gratton 1997)

$$u_f = \lambda \frac{g' h_h^2}{\nu} \quad (\text{A } 1)$$

where  $\lambda$  is a constant. By using (3.3) and (A 1), we find the critical value of the Reynolds number

$$Re_* = \frac{F^2}{\lambda} \approx 50.$$

## REFERENCES

- BEAR, J. 1972 *Dynamics of Fluids in Porous Media*. Elsevier.
- BENJAMIN, T. B. 1968 Gravity currents and related phenomena. *J. Fluid Mech.* **31**, 209–248.
- BOCZAR-KARAKIEWICZ, B., BONA, J. L. & PELCHAT, B. 1991 Interaction of internal waves with the seabed on continental shelves. *Cont. Shelf Res.* **11**, 1181–1197.
- BONNECAZE, R. T., HUPPERT, H. E. & LISTER, J. R. 1993 Particle-driven gravity currents. *J. Fluid Mech.* **250**, 339–369.
- BRITTER, R. E. 1989 Atmospheric dispersion of dense gases. *Ann. Rev. Fluid Mech.* **21**, 317–344.
- BRITTER, R. E. & SIMPSON, J. E. 1978 Experiments on the dynamics of a gravity current head. *J. Fluid Mech.* **88**, 223–240.
- DADE, W. B. & HUPPERT, H. E. 1995 A box model for non-entraining, suspension-driven gravity surges on horizontal surfaces. *Sedimentology* **42**, 453–471.
- DALZIEL, S. B. 1993 Rayleigh-Taylor instability: experiments with image analysis. *Dyn. Atmos. Oceans* **20**, 127–153.
- DALZIEL, S. B. 1995 *DigImage: System Overview*. Cambridge Environmental Research Consultants.
- DULLIEN, F. A. L. 1979 *Porous Media. Fluid Transport and Pore Structure*. Academic.

- FANNELOP, T. K. & WALDMAN, G. D. 1972 Dynamics of oil slicks. *AIAA J.* **10**, 506–510.
- FANNELOP, T. K. & ZUMSTEG, F. 1986 Special problems in heavy-gas dispersion. In *Heavy Gas and Risk Assessment, III* (S. Hartwig), pp. 123–36. D. Reidel.
- FAY J. A. 1969 The spread of oil slicks on a calm Sea. In *Oil on the Sea* (ed. D. P. Hoult), pp. 43–63. Plenum.
- GRATTON, J. & VIGO, C. 1994 Self-similar gravity currents with variable inflow revisited: plane currents. *J. Fluid Mech.* **258**, 77–104.
- GROBELBAUER, H. P., FANNELOP, T. K. & BRITTER, R. E. 1993 The propagation of intrusion fronts of high density ratios. *J. Fluid Mech.* **250**, 669–687.
- GRUNDY, R. E. & ROTTMAN, J. W. 1985 The approach to self-similarity of the solutions of the shallow-water equations representing gravity-current releases. *J. Fluid Mech.* **156**, 39–53.
- GRUNDY, R. E. & ROTTMAN J. W. 1986 Self-similar solutions of the shallow-water equations representing gravity currents with variable inflow. *J. Fluid Mech.* **169**, 337–351.
- HACKER, J., LINDEN, P. F. & DALZIEL S. B. 1996 Mixing in lock-release gravity currents. *Dyn. Atmos. Oceans* **24**, 183–195.
- HOULT D. P. 1972 Oil spreading on the sea. *Ann. Rev. Fluid Mech.* **4**, 341–368.
- HUPPERT, H. E. 1982 The propagation of two-dimensional and axisymmetric viscous gravity currents over a rigid horizontal surface. *J. Fluid Mech.* **121**, 43–58.
- HUPPERT, H. E. & SIMPSON, J. E. 1980 The slumping of gravity currents. *J. Fluid Mech.* **99**, 785–799.
- KEULEGAN, G. H. 1957 An experimental study of the motion of saline water from locks into fresh water channels. *Natl Bur. Stand. Rep.* 5168.
- LIONET, J. & QUOY, O. 1995 Gravity currents over porous media. Internal Rep., DAMTP, University of Cambridge.
- MARINO, B. M., THOMAS, L. P., DIEZ, J. A. & GRATTON, R. 1996 Capillary effects on viscous gravity spreadings of wetting liquids. *J. Colloid Interface Sci.* **177**, 14–30.
- MARINO, B. M., THOMAS, L. P. & GRATTON R. 1997 Shape and size of the current head in creeping flows. *Phys. Rev. E* **55**, 4296–4301.
- MAXWORTHY, T. 1983 Gravity currents with variable inflow. *J. Fluid Mech.* **128**, 247–257.
- MIDDLETON, G. V. 1993 Sediment deposition from turbidity currents. *Ann. Rev. Earth Planet. Sci.* **21**, 89–114.
- ROTTMAN, J. W. & SIMPSON, J. E. 1983 Gravity currents produced by instantaneous releases of a heavy fluid in a rectangular channel. *J. Fluid Mech.* **135**, 95–110.
- SIMPSON, J. E. 1997 *Gravity currents: In the Environment and the Laboratory*, 2nd Edn. Cambridge University Press.
- SIMPSON, J. E. & BRITTER, R. E. 1979 The dynamics of the head of a gravity current advancing over a horizontal surface. *J. Fluid Mech.* **94**, 477–495.
- THORPE, S. A. 1966 Internal gravity waves. PhD dissertation, University of Cambridge.
- WALLACE, B. C. & WILKINSON, D. L. 1988 Run-up of internal waves on a gentle slope in a two-layered system. *J. Fluid Mech.* **191**, 419–442.